



The ‘lightning’ gold nanorods: fluorescence enhancement of over a million compared to the gold metal

Mona B. Mohamed, Victor Volkov, Stephan Link, Mostafa A. El-Sayed *

Laser Dynamics Laboratory, School of Chemistry and Biochemistry, Georgia Institute of Technology, Atlanta, GA 30332-0400, USA

Received 9 November 1999; in final form 29 November 1999

Abstract

Gold nanorods capped with micelles and having an aspect ratio of 2.0–5.4 are found to fluoresce with a quantum yield which is over a million times that of the metal. For rods of the same width, the yield is found to increase quadratically while the wavelength maximum increases linearly with the length. We assign this emission to the electron and hole interband recombination. The increase in the emission yield results from the enhancement effect of the incoming and outgoing electric fields via coupling to the surface plasmon resonance in the rods. This is similar to the previously proposed fluorescence and the Raman enhancement on noble metal rough surfaces. © 2000 Published by Elsevier Science B.V. All rights reserved.

1. Introduction

Nanometer-size particles have received much attention in the recent years due to the tunability of their electronic and hence optical properties with particle size [1,2]. However, not only possible future applications in the areas of optical data storage, ultrafast data communication systems [3] or solar energy conversion [4] have motivated scientists in various fields, but also the question of how bulk-like material properties evolve from the atomic or molecular level with increasing particle size is of great fundamental interest [1–5].

Metallic nanoparticles, especially the noble metals, have mainly been studied because of their strong

optical absorption in the visible caused by the collective excitation of the free electron gas [1,3,5,6]. This coherent electron motion gives rise to the surface plasmon absorption and decays non-radiatively by electron–electron collisions on the order of a few femtoseconds [7,8]. The resonance frequency as well as the width of the plasmon absorption band depend on the nanoparticle size and many theories have been developed to explain the observed experimental behavior [5]. Furthermore, a strong shape dependence of the optical absorption spectrum of metallic nanoparticles is found as the surface plasmon resonance splits into a transverse mode (perpendicular to the long axis of the rod) and a longitudinal mode (parallel to the long rod axis) [6]. The latter depends linearly on the aspect ratio (length divided by the width) of the nanorods [9,10].

Recent time-resolved femtosecond experiments have investigated the excited electron dynamics in metallic nanoparticles [11–19] and found a strong

* Corresponding author. Fax: +1-404-894-0294; e-mail: mostafa.el-sayed@chemistry.gatech.edu

bleaching of the surface plasmon resonance(s) due to the selective heating of the electron gas by a laser pulse. The excitation energy decays mainly non-radiatively via electron–phonon collisions followed by phonon–phonon relaxation with the surrounding medium.

Recently, Wilcoxon et al. [20] reported photoemission from gold nanoclusters with a very small average size (< 5 nm). The photoluminescence was assigned to the radiative recombination of Fermi level electrons and sp- or d-band holes created after photoexcitation. While semiconductor nanoparticles such as CdS and CdSe are well known to show a size-dependent luminescence spectrum [21,22] shifting to higher energies with decreasing cluster size and quantum efficiencies that can reach $> 50\%$ if the surface is highly passivated [23], the observation of fluorescence from metallic nanoparticles and its origin have not been studied in great detail so far.

In this Letter, we report on the luminescence properties of gold nanorods and nanospheres synthesized electrochemically. We observed that while nanodots of 35 nm diameter did not emit, nanorods are found to have fluorescence of quantum efficiency which is 6–7 orders of magnitude higher than that of the metal. Furthermore, its wavelength maximum and quantum efficiency are found to increase linearly with increasing the rod length and the square of the length, respectively. We were able to account for this giant enhancement semiquantitatively by the model of Boyd et al. [24] used to explain fluorescence enhancement from rough surfaces of noble metals by coupling with the local plasmon resonance.

2. Experimental

Using the electrochemical method described by Yu et al. [25], gold nanorods of different lengths were prepared. The electrolysis cell contains an Au plate as cathode and a Pt plate as anode. The electrolyte solution consisted of a hydrophilic cationic surfactant, hexadecyltrimethylammonium bromide, and a hydrophobic cationic co-surfactant, tetradecylammonium bromide or tetraoctylammonium bromide. The electrolysis was carried out under ultrasonication with an applied current of 5 mA and at a temperature of 42°C for ~ 45 min. The length of the

gold nanorods depends on the ratio between the surfactant and the co-surfactant concentration and the amount of Ag^+ ions added as a catalyst in the solution.

The size distribution of the nanorods was determined by analysis of the transmission electron microscopic (TEM) images obtained by using a Hitachi HF-2000 field emission TEM operating at 200 kV. From the enlarged TEM pictures of evaporated drops of the sample solution on a carbon covered copper grid, the size distribution was determined by counting at least 300 particles. As an example, the TEM image of dried gold nanorods of average aspect ratio 3.3 and its size distribution are shown in Fig. 1. We synthesized and studied samples with aspect ratios of 2.0, 2.6, 3.3, 4.3, and 5.4, most of them have comparable width of ~ 20 nm.

The electronic absorption spectra were recorded on a Beckman DU 650 spectrophotometer. The fluorescence was recorded using a Shimadzu RF-5301 PC spectrofluorophotometer by exciting the gold

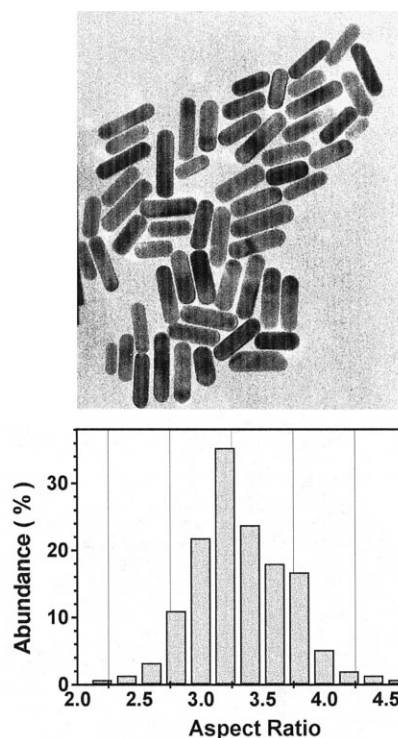


Fig. 1. TEM image of gold nanorod solution and its aspect ratio distribution.

nanorods samples of different aspect ratios at 480 nm. The quantum yield was measured by comparing the emission intensity from gold nanorods with that from Rhodamine 6-G having the same optical density at the exciting wavelength of 480 nm.

3. Results and discussion

The optical absorption properties of gold nanoparticles in the visible range are very much dictated by the effect of the boundary conditions of the coherent electron oscillations and also due to the interband $d \rightarrow sp$ electronic transitions. The surface plasmon absorption spectra of gold nanospheres is characterized by a strong absorption band in the visible region at ~ 520 nm. Very small gold particles (< 2 nm) as well as bulk gold do not show this absorption [5,6]. The absorption spectrum of gold nanorods is characterized by two bands [9,10]. The short-wavelength band is located at around 520 nm and is attributed to the transverse surface plasmon resonance. This band has some contribution from the spherical gold nanoparticles present in the solution, and it shifts only slightly to shorter wavelength with increasing the average aspect ratio of the nanorods. The maximum of the second absorption band appears at longer wavelength and corresponds to the longitudinal surface plasmon resonance and increases with increasing the aspect ratio. Absorption spectra of rods of different average aspect ratios are shown in Fig. 2.

Fig. 3 summarizes the observed features of the emission from the gold nanorod solutions studied, having aspect ratios of 2, 2.6, 3.3, 4.3, and 5.4 with similar average width of 20 nm. It is obvious that as the length increases, the emission wavelength maximum increases linearly as shown in Fig. 3a. The measured quantum efficiency is also found to increase with the square of the length as shown in Fig. 3b. The measured quantum efficiency is on the order of 10^{-4} – 10^{-3} , which is 6–7 orders of magnitude higher than that observed for the emission from the metal surface.

The observed wavelength region (548–590 nm) eliminates the origin of this emission to be from the micelle molecules. The excitation wavelength (480 nm) is in the region of the transverse surface plas-

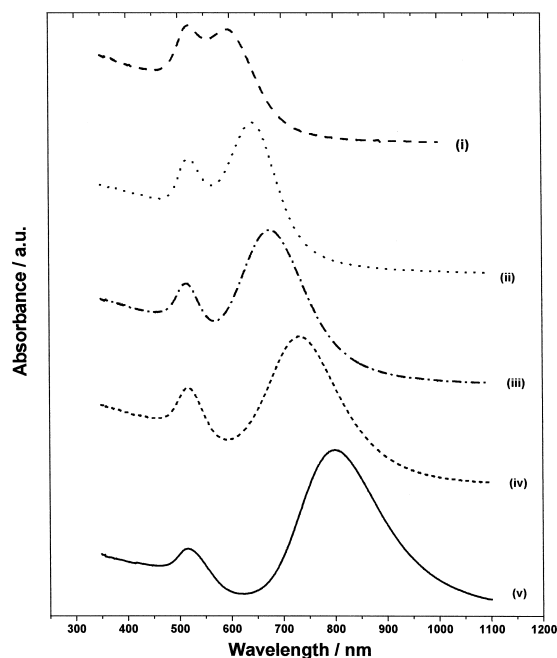


Fig. 2. The absorption spectra i, ii, iii, iv, and v for gold nanorods of average aspect ratios 2.0, 2.6, 3.3, 4.3, and 5.4, respectively. The longitudinal surface plasmon absorption band of gold nanorods mainly depends on the average aspect ratio.

mon absorption band, which is not sensitive to the length of the rod. The longitudinal surface plasmon absorption red-shifts linearly with the rod length. However, this absorption is at much longer wavelength than the observed emission (see Fig. 2). This eliminates assigning the emission to surface plasmon radiative relaxation. The other absorption occurring in this region is the $d \rightarrow sp$ intraband transition found in the metal.

Photoluminescence from copper and gold metals was first observed by Mooradian [26], and has been used extensively in characterizing carrier relaxation and the band structure of metals [26–31]. They found that the emission spectra (excited by a 2 W cw laser beam at 488 nm) is totally unpolarized and did not depend on the polarization of the incident laser beam. The emission peak was centered near the interband absorption edge of the metals and was attributed to direct radiative recombination of the conduction band electrons with holes in the d -band that have been scattered to momentum states less than the Fermi momentum. The quantum efficiency

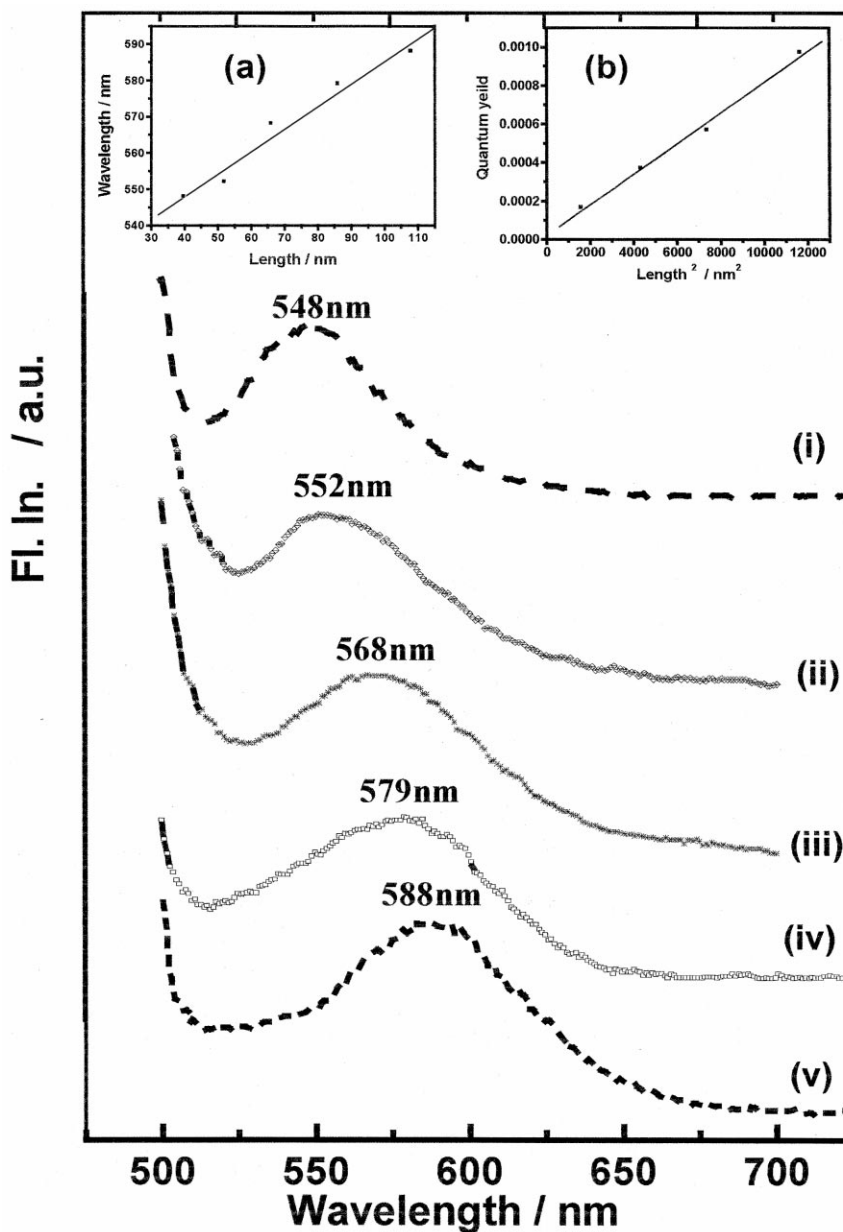


Fig. 3. The emission spectra i, ii, iii, iv, and v for gold nanorods of average aspect ratios 2.0, 2.6, 3.3, 4.3, and 5.4, respectively. Most of them have comparable width of ~ 20 nm. It is shown that the emission spectra of gold rods depend on the average aspect ratio. By increasing the aspect ratio, the wavelength maximum of the emission band increases. The inset (a) shows that the wavelength maximum of the emission band depends linearly on the average aspect ratio of the gold nanorods. The inset (b) shows that the quantum efficiency of this emission is linearly dependent on the square of the length of the rods (L^2).

was found to be on the order of 10^{-10} . However, many of the essential details of this mechanism, such

as the excited electron and hole population distributions and the specific regions in the Brillouin zone

where the recombination takes place have not been discussed. After almost a couple of decades, Boyd et al. [24] did a complete experimental study of this phenomenon using a single-photon induced luminescence technique. They used a simple calculation to determine the relation between the spectral peaks and the interband recombination at selected symmetry points in the Brillouin zone. They also studied the effect of roughness on the surface local fields and on the emission spectra. A theoretical model to explain the radiative recombination in noble metals was developed by Apell et al. [30]. It was pointed out that there was slight overlap between the sp-conduction band and the d-valence band as demonstrated by the Stokes shift of the luminescence band [30].

Excitation of the gold nanorods at 480 nm leads to excitation of the surface plasmon coherent electronic motion as well as the d-electrons. Relaxation of these electronic motions followed by the recombination of the sp-electrons with holes in the d-band we believe leads to the observed emission. Because of the rod shape, both of the exciting and the emission fields are enhanced to give rise to the observed increase in the emission quantum efficiency and the maximum of the emission band by increasing the rod length. The theory of the local field was well developed and proven to be useful in describing the induced linear or nonlinear optical responses from rough metal surfaces [32]. Application of the local field theory to rough Cu surface considered as an ensemble of independent hemispheres led Boyd et al. [24] to build a theoretical model, which shows how the emission intensity and band position are sensitive to the aspect ratio of the hemispheres. Below we used this model for the gold nanorods and show how it could be used to describe our experimental observations on the trends of the red-shift of the emission band and increasing the quantum efficiency with increasing the average aspect ratio (length) of the gold nanorods.

According to the theoretical studies of the photoinduced luminescence [24] and the surface enhanced second-harmonic generation [32] from rough surfaces of noble metals, the incoming and outgoing fields are proposed to be enhanced via coupling to the local plasmon resonances. The rough surface is assumed to be a random collection of noninteracting hemispheroids of height a , radius b and volume V

$= \frac{4}{3}\pi ab^2$. The local field correction factor within the spheroid $L(\omega)$ is then given by [24,32]:

$$L(\omega) = \frac{L_{\text{LR}}}{\varepsilon_1(\omega) + i\varepsilon_2(\omega) - 1 + L_{\text{LR}} \left(1 + \frac{4\pi^2 iV [1 - \varepsilon_1(\omega) - i\varepsilon_2(\omega)]}{3\lambda^3} \right)}. \quad (1)$$

L_{LR} is called the lightning-rod factor and is defined as $L_{\text{LR}} = 1/A$, where:

$$A = \frac{1}{1 - \frac{\xi Q_1'(\xi)}{Q_1(\xi)}},$$

$$\xi = \frac{1}{\sqrt{1 - \left(\frac{b}{a}\right)^2}},$$

$$Q_1(\xi) = \frac{\xi}{2} \ln \left(\frac{\xi + 1}{\xi - 1} \right) - 1,$$

and

$$Q_1'(\xi) = \frac{dQ_1(\xi)}{d\xi}.$$

$\varepsilon(\omega) = \varepsilon_1(\omega) + i\varepsilon_2(\omega)$ is the frequency-dependent complex dielectric function of the metal and was taken from Ref. [33], while λ is the optical wavelength. With Eq. (1) the single-photon luminescence power P_1 can be calculated [24] for excitation and emission energies $h\omega_{\text{exc}}$ and $h\omega_{\text{em}}$

$$P_1 = 2^4 \beta_1 |E_0|^2 V |L^2(\omega_{\text{exc}}) L^2(\omega_{\text{em}})|, \quad (2)$$

where E_0 is the incident electric field and β_1 is a proportionality constant, which includes the intrinsic luminescence spectrum of the gold.

Assuming that the luminescence of the gold nanorods is similarly enhanced due to the local field factor, $P_1/|E_0|^2 \beta_1$ was calculated as a function of the gold nanorod length with constant width of 20 nm and the emission wavelength for a fixed volume (for our particles, $a = 86$ nm; $b = 10$ nm; $R = 4.3$) and exciting at 500 nm. The result is shown in

Fig. 4. The resonant luminescence power increases with increasing nanorod length (lightning-rod effect) and shifts to longer emission wavelength. Furthermore, note that $P_1/|E_0|^2\beta_1$ is on the order of 10^7 . Both the red-shift of the photoluminescence of the gold nanorods and the magnitude of the luminescence power due to the local field correction factor are in good agreement with experimental results.

2-D plots of the results shown in Fig. 4 are given in Fig. 5 demonstrating the relationship between the luminescence power and the nanorod length (a) and the emission maximum of the luminescence power and the nanorod length (b). The luminescence power increases linearly with the square of the length of the rod while a linear dependence on the length is found for the emission maximum. These results are in good agreement with the experimental observations shown in Fig. 3a and b, respectively. The above agreement between theory and experiment strongly supports our assignment of the origin of the fluorescence from gold nanorods and that suggests that the mechanism of its large increase in its efficiency in these rods is the great enhancement of the incoming exciting light

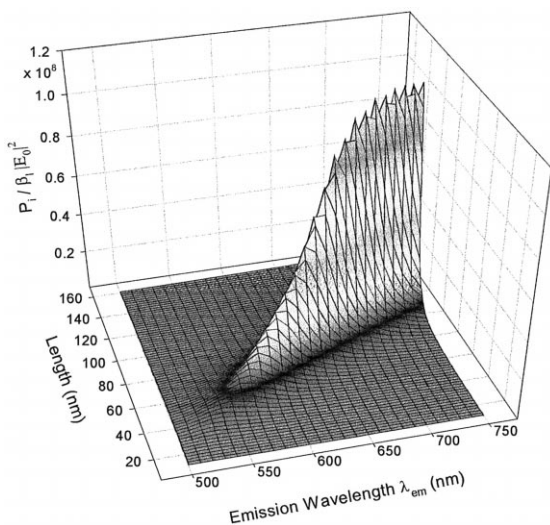


Fig. 4. Calculated single-photon luminescence power $P_1/|E_0|^2\beta_1$ emitted from a gold nanorods as a function of the emission wavelength and the nanorod length (constant width of 20 nm). The excitation wavelength was chosen to be 500 nm, while the volume V was fixed according to a length of 86 nm and a width of 20 nm.

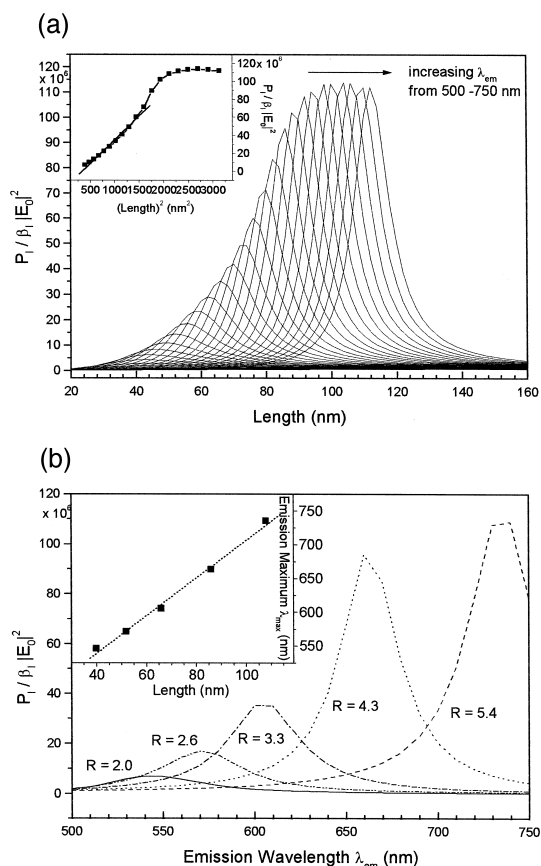


Fig. 5. 2-D plot of $P_1/|E_0|^2\beta_1$ as a function of the gold nanorod length for different emission wavelength between 500 and 750 nm in steps of 10 nm. The inset shows that the single-photon luminescence power increases linearly with the square of the nanorod length in the range of 20 to ~ 80 nm. This is in agreement with the experimental results (see Fig. 3). (b) 2-D plot of $P_1/|E_0|^2\beta_1$ as a function of the emission wavelength for the aspect ratios of the samples used in the experimental studies. The emission maximum of the luminescence power scales linearly with nanorod length as shown in the inset. This trend is also found experimentally (see Fig. 3).

and the outgoing emitted light via the excitation of the surface plasmon resonance.

Acknowledgements

This work was supported by the National Science Foundation, Grant No. CHE-9727633. M.B.M. likes to thank the Egyptian GM for a Ph.D. scholarship. S.L. thanks Molecular Design Institute (MDI), Georgia Institute of Technology for financial support.

References

- [1] A. Henglein, *J. Phys. Chem.* 97 (1993) 8457.
- [2] A.P. Alivisatos, *J. Phys. Chem.* 100 (1996) 13226.
- [3] G. Schmid (Ed.), *Clusters and Colloids: From Theory to Application*, VCH, Weinheim, 1994.
- [4] M. Graetzel, in: R.A. Mackay, J. Texter (Eds.), *Electrochemistry in Colloids and Dispersions*, VCH, Weinheim, 1992.
- [5] U. Kreibig, M. Vollmer, *Optical Properties of Metal Clusters*, Springer, Berlin, 1995.
- [6] G.C. Papavassiliou, *Prog. Solid State Chem.* 12 (1980) 185.
- [7] U. Kreibig, M. Gartz, A. Hilger, *Ber. Bunsen-Ges.* 48 (1997) 18178.
- [8] S. Link, M.A. El-Sayed, *J. Phys. Chem. B* 103 (1999) 4212.
- [9] B.M.I.v.d. Zande, M.R. Bohmer, L.G.J. Fokkink, C. Schonenberger, *J. Phys. Chem. B* 101 (1997) 8520.
- [10] S. Link, M. Mohamed, M.A. El-Sayed, *J. Phys. Chem. B* 103 (1999) 3073.
- [11] T.S. Ahmadi, S.L. Logunov, M.A. El-Sayed, *J. Phys. Chem.* 100 (1996) 8053.
- [12] S. Link, C. Burda, M.B. Mohamed, B. Nikoobakht, M.A. El-Sayed, *Phys. Rev. B* (1999), in press.
- [13] M. Perner, P. Bost, G.v. Plessen, J. Feldmann, U. Becker, M. Mennig, H. Schmidt, *Phys. Rev. Lett.* 78 (1997) 2192.
- [14] J.K. Hodak, I. Martini, G.V. Hartland, *J. Phys. Chem. B* 102 (1998) 6958.
- [15] J.-Y. Bigot, J.-C. Merle, O. Cregut, A. Daunois, *Phys. Rev. Lett.* 75 (1995) 4702.
- [16] T.W. Roberti, B.A. Smith, J.Z. Zhang, *J. Chem. Phys.* 102 (1995) 3860.
- [17] N. Del Fatti, C. Flytzanis, F. Vallee, *Appl. Phys. B* 68 (1999) 433.
- [18] M.J. Feldstein, C.D. Keating, Y.-H. Liao, M.J. Natan, N.F. Scherer, *J. Am. Chem. Soc.* 119 (1997) 6638.
- [19] R.D. Averitt, S.L. Westcott, N.J. Halas, *Phys. Rev. B* 58 (1998) 10203.
- [20] J.P. Wilcoxon, J.E. Martin, F. Parsapour, B. Wiedenman, D.F. Kelley, *J. Chem. Phys.* 108 (1998) 9137.
- [21] M.L. Steigerwald, A.P. Alivisatos, J.M. Gibson, T.D. Harris, R. Kortan, A.J. Muller, A.M. Thayer, T.M. Duncan, D.C. Douglas, L.E. Brus, *J. Am. Chem. Soc.* 110 (1988) 3046.
- [22] L. Spanhel, M. Haase, H. Weller, A. Henglein, *J. Am. Chem. Soc.* 109 (1987) 5649.
- [23] B.O. Babbouni, J. Rodriguez-Viejo, F.V. Mikulec, J.R. Heine, H. Mattoussi, R. Ober, K.F. Jensen, M.G. Bawendi, *J. Phys. Chem. B* 101 (1997) 9463.
- [24] G.T. Boyd, Z.H. Yu, Y.R. Shen, *Phys. Rev. B* 33 (1986) 7923.
- [25] Y. Yu, S. Chang, C. Lee, C.R.C. Wang, *J. Phys. Chem. B* 101 (1997) 6661.
- [26] A. Mooradian, *Phys. Rev. Lett.* 22 (1969) 185.
- [27] D.G. Whittle, E. Burstein, *Bull. Am. Phys. Soc.* 26 (1981) 777.
- [28] M. Moshovits, *Rev. Mod. Phys.* 57 (1985) 783.
- [29] J.P. Heritage, J.G. Bergman, A. Pinczuk, J.M. Worlock, *Chem. Phys. Lett.* 67 (1979) 229.
- [30] P. Apell, R. Monreal, *Phys. Scr.* 38 (1988) 174.
- [31] V.G. Plekhanov, T.V. Siliukova, *Sov. Phys. Solid State* 32 (1990) 1268.
- [32] G.T. Boyd, T. Rasing, J.R.R. Leite, Y.R. Shen, *Phys. Rev. B* 30 (1984) 519.
- [33] P.B. Johnson, R.W. Christy, *Phys. Rev. B* 6 (1972) 4370.